Coalesced Core/Shell Latex Films under Elongation Imaged by Atomic Force Microscopy

S. Lepizzera, M. Scheer, C. Fond, T. Pith, M. Lambla, and J. Lang*

Institut Charles Sadron (CRM-EAHP), CNRS-ULP Strasbourg, 6 rue Boussingault, 67083 Strasbourg Cédex, France

Received May 20, 1996; Revised Manuscript Received October 4, 1996[⊗]

ABSTRACT: Atomic force microscopy has been used to image deformed latex films. The films were made from core/shell latex particles having a soft shell and a hard core so that when the films were formed, the continuous phase was composed of the shell polymer in which the hard cores formed long range hexagonal orderings. Upon small amounts of film elongation, linear necklaces of core particles, perpendicular to the elongation direction, were observed at the surface of the films. This observation, which is mainly due to matrix deformation and has been analyzed theoretically in the companion paper (preceding paper in this issue), can be easily understood. When the film is elongated, it becomes thinner in the direction perpendicular to the elongation; as a result, the core particles are pushed together in the direction perpendicular to the elongation, whereas, at the same time, the core particles are pulled apart along the direction of elongation. However, as the elongation increases further, AFM images show that, besides the matrix deformation process, another deformation mechanism, which is a geometrical rearrangement of the core particles, appears. The response of the film to the strain is then characterized by the appearance of breaks in the linear necklace of core particles, which now form zigzags or chevrons. Such a geometrical rearrangement of the core particles was anticipated from the failure of the theoretical analysis to account for the experimental strain−stress curves at large film elongations. Therefore, future theoretical analysis of the mechanical behavior at finite strain of coalesced core/shell latex films should take into account both deformation mechanisms.

Introduction

In the first part of this work,[1] two approaches were used to try to describe the uniaxial deformation at finite strain of coalesced core/shell latex films based on a hard core and a soft shell. After latex film formation, biphasic films having a soft matrix with regularly distributed hard inclusions are obtained. The hard cores of the original particles stay intact and form long range hexagonal domains, as shown in Figure 1A. These hard cores are supposed to be undeformable under uniaxial traction, whereas the soft shells form a deformable matrix (Figure 1B). It has been shown[1] that matrix deformation alone cannot account for the extent of film elongation observed experimentally for elongations above 1.3. It is proposed[1] that, besides matrix deformation, a geometrical rearrangement of the hard cores might occur within the film, upon uniaxial deformation. Atomic force microscopy (AFM) has been used to test this assumption. As will be seen, besides matrix deformation, a second mechanism has been observed with this technique. It corresponds to a geometrical rearrangement of the core particles, which tend to align in rows along the elongation direction (Figure 1C).

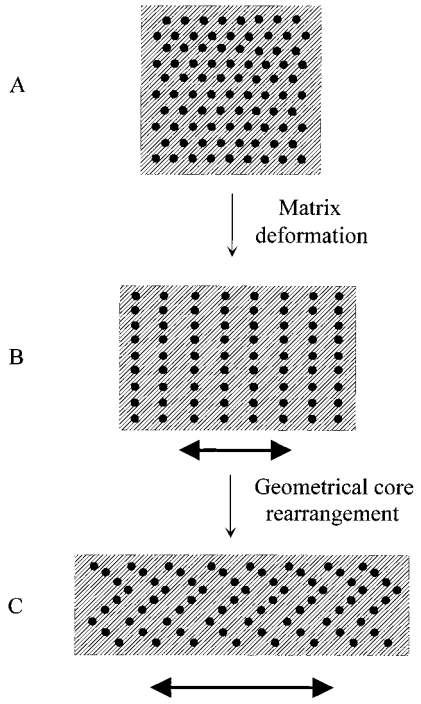

Figure 1. Schematic representation of the core/shell latex films studied, after film formation at 23 °C: (A) undeformed film; (B) film with an elongation below 1.3; (C) film with an elongation above 1.3. The shell-polymer forms the continuous phase (hatched) and the cores (black dots) stay intact. Double arrows indicate the direction of film elongation.

Materials and Method

Latex Synthesis. Two types of core/shell particles have been used in this study. They were prepared by a two-step semicontinuous emulsion polymerization, using potassium persulfate as initiator in the first step (core) and a redox reaction in the second step (shell). The core is made of poly(methyl methacrylate) (PMMA), and the shell, of poly(butyl acrylate-*co*-methyl methacrylate-*co*-acrylic acid). The origin of the various compounds used and a detailed description of the synthesis are fully described elsewhere.[2] The main characteristics of these latexes are given in Table 1. It is worth noticing that the two types of core/shell particles differ by the T_g of the shell, and by the relative weight ratio between the core and the shell. As indicated in Table 1, the particles with the highest T_g of their shell also have the highest shell/core weight ratio. Thus, the two types of films investigated are characterized either by a matrix with a relatively low T_g and a small volume (made from CS1) or by a matrix with a higher T_g and a larger volume (made from CS2). The main idea was to check if these two types of films, which both have good mechanical resistance, experience the same deformation mechanisms under elongation.

[⊗] Abstract published in *Advance ACS Abstracts,* November 1, 1997.

S0024-9297(96)00730-9 CCC: $14.00

Table 1. Latex Characteristics: Symbol Used in the Text, Composition, Core/Shell Weight Ratio, T_g of the Shell, Particle Diameter, D_p, Measured by Quasi-Elastic Light Scattering (QELS) and AFM, and Shell Thickness, e, for the Latexes Used[a]

latex	chemical composition (concn, wt %) core	shell	core/shell wt ratio	shell T_g (°C)	particle diameter ($D_p = 2R_p$, nm) QELS	AFM	theoretical shell thickness (e, nm)	e/R_p
CS1	PMMA (100)	poly(MMA-co-BA-co-AA) (39 (MMA), 59 (BA), 2 (AA))	42/58	−4	255	220	32	0.25
CS2	PMMA (100)	poly(MMA-co-BA-co-AA) (48 (MMA), 50 (BA), 2 (AA))	18/82	9	330	330	72	0.44

[a] MMA, BA, and AA stand for methyl methacrylate, butyl acrylate, and acrylic acid, respectively.

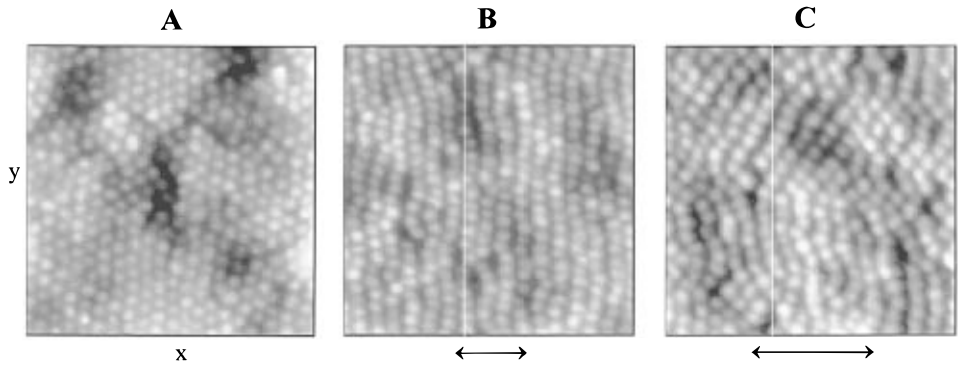

Figure 2. AFM top views of the CS1 latex film: (A) undeformed film; (B) film with an elongation equal to 1.2 ± 0.04; (C) film with an elongation equal to 1.35 ± 0.07. Film elongation is along the *x*-axis, as indicated by the double arrows. Size of the images: 4 μm × 4 μm.

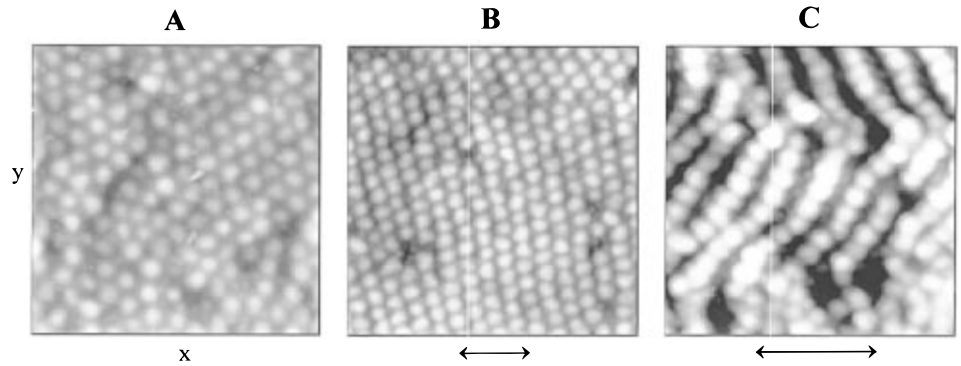

Figure 3. AFM top views of the CS2 latex film: (A) undeformed film; (B) film with an elongation below 1.05; (C) film with an elongation equal to 2 ± 0.2. Film elongation is along the *x*-axis, as indicated by the double arrows. Size of the images: 4 μm × 4 μm.

Film Preparation. Films to be imaged were prepared by pouring a small quantity of the latex dispersion on glass plates, and then allowing them to dry under a constant humidity (60 ± 5%) at 23 ± 2 °C for more than 24 h. During this period of time the shell regions of the particles fuse together to form a continuous matrix. Translucent and crack-free films were thus obtained. Films were next cut in small pieces (8 × 6 mm^2) to be used in the AFM. Films to be imaged without deformation were simply glued on a small magnetic disk (diameter = 1.2 cm), which was placed on the top of the piezoelectric translator used to scan the sample under the tip. Films to be imaged under deformation were prepared in two different ways. They were either glued by their extremities under elongation on a mica plate fixed on a magnetic disk or mounted on a home-made device that allows the film to be imaged under various elongations. Thus, in both ways, AFM images the surface morphology of the films under strain and not of the relaxed films after strain. The elongation device is sufficiently small to be directly handled under the AFM. However, its height (4 mm) is not negligible and one has to take into account the separation distance between the translator and the device top surfaces and to correct the *x* and *y* values (which correspond to scans in the plane of the sample) given by the AFM software.[3]

Atomic Force Microscopy. AFM observations were performed with a Nanoscope III microscope from Digital Instruments, Inc., Santa Barbara, CA, equipped with a modified version of Nikon's model MM-11U optical microscope, which allows prelocalization of the area of interest. It also allows the measurement of the elongation of the film when the elongation device is directly placed on the top of the translator. The AFM was used in the tapping mode at a frequency close to 350 kHz. The spring constant of the cantilever was around 40 N m^{-1}. A piezoelectric translator that can scan a maximum surface of 12.5 × 12.5 μm^2, was used. Scans were operated in the height mode, which means that the force exerted on the film surface by the cantilever tip was kept constant by varying the height of the sample relative to the tip through an electronic feedback loop. No filter treatment was done to the images and all measurements were done in ambient air, i.e., at a temperature much below the T_g (110 °C) of the core.

Results and Discussion

Figures 2 and 3 show top views of various film surfaces. The plane of these figures represents the $x-y$ scans of the tip at the film surface. The z scale representation on the AFM images is achieved by using a color scale, which is gray on our images. The darker the gray, the lower the value of z. Thus, the lighter parts of these images represent the more elevated part of the film surface. Figure 2 is for CS1 and Figure 3 for CS2. Figures 2A and 3A are images of the surface of the films before elongation. These images show that

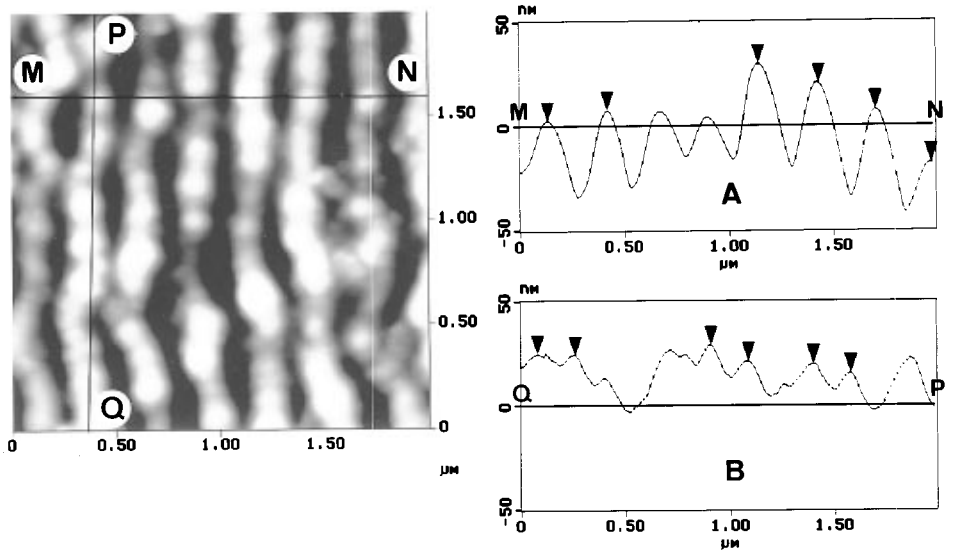

Figure 4. AFM top view and cross section profile along lines MN (cross section A) and PQ (cross section B) for a film of CS1 under elongation. The direction of elongation is along the horizontal *x*-axis.

the matrix of the films forms a continuous phase between the core particles that are clearly visible. The continuous phase is made of the polymer that originally formed the shell of the particles, whereas the lighter parts that appear as more or less spherical particles are in fact the core of the original core/shell particles. Recall that the T_g of the shell (see Table 1) is below the ambient temperature whereas the T_g of the core (110 °C) is much above it. The cores in Figures 2A and 3A form well-known hexagonal domains (schematically illustrated in Figure 1A), which indicates that the original core/shell particles were rather monodisperse in size.

Figures 2B and 3B show the surface of the films under elongation. The elongation is parallel to the *x*-axis, as indicated by the arrows drawn on the figures. Image 2B has been obtained with an elongation of about 1.2 ± 0.04, and image 3B with an elongation of less than 1.1. In both cases one observes an alignment of the particles (in fact the core of the original particles), which forms some kind of linear "necklaces", all oriented in the same direction, namely perpendicular to the direction of elongation. Compared to the original films (images A), the mean distance between the particles along a necklace of particles has decreased, whereas the mean distance between the particles belonging to adjacent necklaces has increased. This modification is illustrated schematically in Figure 1B. This result is easily explained. When the film is elongated along the *x* direction, its width along the *y* direction is reduced. As a result, the particles are pulled apart along the *x* direction, and pushed closer in the *y* direction. This process, which arises only from matrix deformation, has been modeled and analyzed in detail in the preceding paper.[1]

As the elongation of the film increases, the AFM images show that a geometrical rearrangement of the core particles occurs. Images 2C and 3C correspond to elongations of the films equal to 1.35 ± 0.07 and 2 ± 0.2, respectively. Images 2C and 3C are quite different from images 2B and 3B. They show that the necklaces of particles at the film surface are no longer perpendicular to the direction of elongation but tend to orient in the direction of film elongation. Moreover, breaks occur in the linear necklaces. They then form a geometrical arrangement that looks like chevrons. Formation of chevrons is more apparent in image 3C. This deformation is schematically depicted in Figure 1C. Thus, this result indicates that above a certain value of the elongation, the deformation of the matrix is not the only mechanism occurring. A geometrical rearrangement of the core particles, visible here at the surface of the film, but which probably also occurs inside the film, as discussed shortly below, is necessary.

All the above results concern deformations that have been observed at the surface of the film. One can therefore wonder if the same deformations occur in the bulk. Although we have not, at the present time, direct evidence that the observations made at the surface of the film reflect what is happening inside the film, there are two main arguments that indicate that this is, indeed, probably the case: (i) For small values of the elongation the model of matrix deformation developed in the previous paper[1] accounts for the mechanical stress−strain data. This model has been developed to account for the deformation in the bulk but corresponds precisely to what is seen by AFM in Figures 2B and 3B. (ii) We have seen in Figures 2C and 3C that for large elongations there is a reorientation of the core particles in the direction in which the film is elongated. Similar results were obtained from small angle neutron scattering (SANS) measurements done on another latex system where "strong" dispersed particles were surrounded by a "weak" matrix.[4] Indications were obtained that a change in the structure of the lattice, and not only of the unit cell, occurs as the film elongation increases. This change, which is observed inside the film by SANS, seems to involve a process in which neighboring particles "avoid each other" by slipping along the stretching direction. This is exactly what is observed at the surface of our films by AFM. This result tends also to indicate that the rearrangement observed at the surface of our films may well reflect what is happening inside the film.

The AFM top view shown in Figure 4 is for a CS1 film under elongation. Two cross sections, A and B, taken along lines MN and PQ represented on the top view image, are also shown in this figure. The line MN and the cross section A correspond to a direction parallel to the direction of film elongation, whereas the line PQ and the cross section B correspond to a direction perpendicular to it. One sees that the corrugation along

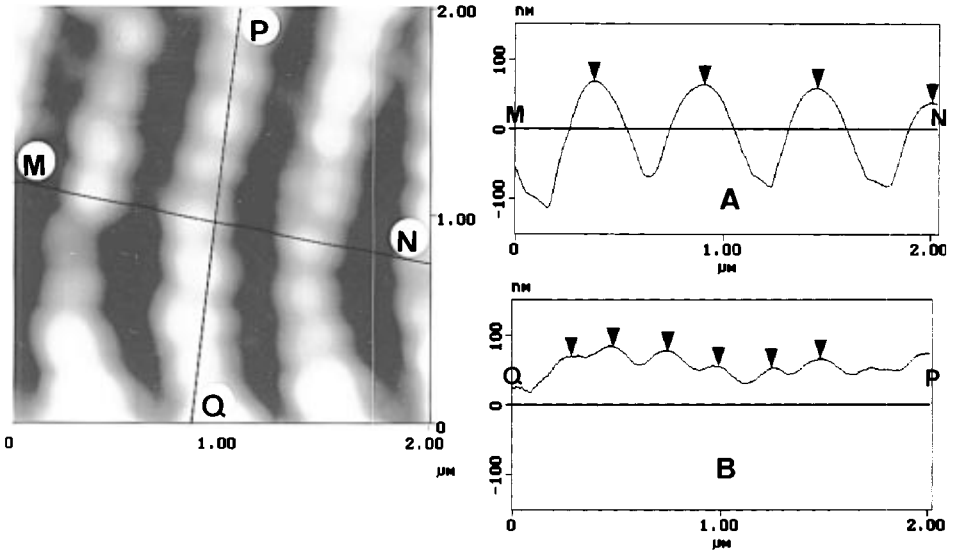

Figure 5. AFM top view and cross section profile along lines MN (cross section A) and PQ (cross section B) for a film of CS2 under elongation. The direction of elongation is along the horizontal *x*-axis.

Table 2. Mean Distance, d_p, between the Core-Particles in the Undeformed Films, Mean Distance between the Core-Particles in the Direction Parallel, $d_{||}$, and Perpendicular, $d_\perp$, to the Direction of Elongation, and Film Elongation, $\lambda_{||}$ and $\lambda_\perp$, Calculated from the Film Deformation Parallel and Perpendicular to the Direction of Elongation

latex	d_p (nm)	$d_{||}$ (nm)	$\lambda_{||}$[a]	$d_\perp$ (nm)	$\lambda_\perp$[b]
CS1	220	285	1.3	180	1.5
CS2	330	545	1.65	250	1.7

[a] $\lambda_{||}$ corresponds to film elongation calculated from d_p and $d_{||}$: $\lambda_{||} = d_{||}/d_p$. [b] $\lambda_\perp$ corresponds to film elongation calculated from d_p and $d_\perp$: $\lambda_\perp = (d_p/d_\perp)^2$.

line MN is more significant than along line PQ. This is due to the fact that, upon elongation, the particles are pulled apart along line MN and pushed closer together along line PQ. The triangles in the cross sections A and B simply indicate the center of some of the core particles. The mean distance, d, between the center of the core particles in cross sections A ($d_{||}$) and B ($d_\perp$) are compared in Table 2 to the mean distance, d_p, measured between particles in the undeformed film. As expected, the value of $d_{||}$ is larger, and the value of $d_\perp$ lower, than d_p. From d_p and $d_{||}$ values, the elongation, $\lambda_{||}$, of the film, equal to $d_{||}/d_p$, can be calculated and compared to the value of the elongation $\lambda_\perp$, equal to $(d_p/d_\perp)^2$, calculated from the film deformation in the direction perpendicular to the film elongation direction. For no volume change upon deformation, $\lambda_{||}$ and $\lambda_\perp$ should be equal. The values of $\lambda_{||}$ and $\lambda_\perp$ are given in Table 2. The agreement between the values found, 1.3 for $\lambda_{||}$ and 1.5 for $\lambda_\perp$, is not perfect, but is within the range of the experimental error. Part of the difference can also come from film inhomogeneity. Better agreement is found in the case of CS2, as seen now.

Figure 5 is for a CS2 film under elongation. As in Figure 4, line MN and cross section A correspond to a direction approximately parallel to the direction of film elongation, whereas line PQ and cross section B correspond to a direction approximately perpendicular to the direction of film elongation. Here again, as expected, the value of $d_{||}$ is larger, and the value of $d_\perp$ lower, than d_p. The corrugation is also higher along line MN than along line PQ. Finally, close agreement is found here between $\lambda_{||}$ (1.65) and $\lambda_\perp$ (1.7).

The AFM images shown in this work illustrate the possibility of using this technique for the study of film deformation. The main merit of this work is to show that for large elongation a rearrangement of the hard core particles occurs, in addition to matrix deformation. However, there are certain issues that will be studied in the future. One is to determine if there is a critical film elongation value above which a rearrangement of the core particles appears, or does this process occur progressively as the film elongation increases. Another will be to examine the effect of the core-particle concentration on the film deformation, mainly for large elongation. Indeed, for high concentrations of core particles in the film, the contacts between the cores occur earlier upon film elongation than when the concentration of the core particles is low. This might have an appreciable effect on the core-particle rearrangement. Finally, it would be useful and instructive to quantify the observed core particles rearrangement, by measuring the mean number of particles present in the arms of the chevrons or the mean angle between the arms that form the chevrons, for different values of film elongation.

Conclusion

We have shown that AFM can be used to study the deformation of multiphasic films. A special device has been built for this purpose. The biphasic films studied here were made from core/shell particles having a soft shell and a hard core. The core, which has a high T_g, keeps its integrity once the film is formed at ambient temperature. As the deformation of the film begins, linear necklaces of core particles are formed, which are oriented perpendicularly to the film elongation direction. The formation of these linear necklaces is easy to explain. Upon film elongation, the core particles are pushed closer together (film becomes thinner) in the direction perpendicular to the film elongation direction, whereas the core particles are pulled apart in the parallel direction. This process, due simply to matrix deformation, has been analyzed theoretically in the previous paper.[1] As the elongation increases further, a geometrical rearrangement of the core particles occurs inside the film. This geometrical rearrangement is apparent at the film surface where breaks in the linear necklaces of the core particles develop. These necklaces

of core particles then form zigzags or chevrons. This result proves that for large elongation a simple deformation of the continuous phase is not the only mechanism responsible for film deformation. There is also a geometrical rearrangement of the core particles within the film. The analysis of latex film deformation may be greatly improved, for large deformation, if this geometrical rearrangement is taken into account in future theoretical calculations.

Acknowledgment. The authors thank Mr. Rémy Hecht (ICS-CRM Strasbourg) for the construction of the sample elongation device which could be mounted on the AFM. S. L. thanks L'Oréal for its financial support.

References and Notes

(1) Lepizzera, S.; Pith, T.; Fond, C.; Lambla, M. *Macromolecules* **1997**, *30*, 7945.
(2) Lepizzera, S. Ph.D. Thesis, Université Louis Pasteur, Strasbourg, 1996.
(3) Snétigny, D.; Vancso, G. J. *Langmuir* **1993**, *9*, 2253.
(4) Rharbi, Y.; Boué, F.; Joanicot, M.; Cabane, B. *Macromolecules* **1996**, *29*, 4346.

MA960730K